CLEO CONF 96-04
ICHEP96 PA07-068

A Measurement of the Michel Parameters in Leptonic Decays of the Tau

CLEO Collaboration

(July 18, 1996)

Abstract

We have measured the spectral shape Michel parameters ρ and η using leptonic decays of the τ recorded by the CLEO II detector. Assuming lepton $(e-\mu)$ universality, we find $\rho^{\tau}_{e\mu} = 0.739 \pm 0.016$ (stat) $\pm$ 0.013 (syst) and $\eta^{\tau}_{e\mu} = 0.025 \pm 0.074$ (stat) $\pm$ 0.066 (syst). Each of these measurements has precision comparable to the corresponding world average.

A. Bellerive,[1] D. I. Britton,[1] R. Janicek,[1] D. B. MacFarlane,[1] K. W. McLean,[1]
P. M. Patel,[1] A. J. Sadoff,[2] R. Ammar,[3] P. Baringer,[3] A. Bean,[3] D. Besson,[3] D. Coppage,[3]
C. Darling,[3] R. Davis,[3] N. Hancock,[3] S. Kotov,[3] I. Kravchenko,[3] N. Kwak,[3] S. Anderson,[4]
Y. Kubota,[4] M. Lattery,[4] J. J. O'Neill,[4] S. Patton,[4] R. Poling,[4] T. Riehle,[4] A. Smith,[4]
V. Savinov,[4] M. S. Alam,[5] S. B. Athar,[5] Z. Ling,[5] A. H. Mahmood,[5] H. Severini,[5]
S. Timm,[5] F. Wappler,[5] A. Anastassov,[6] S. Blinov,[6,*] J. E. Duboscq,[6] R. Fulton,[6]
D. Fujino,[6] K. K. Gan,[6] T. Hart,[6] K. Honscheid,[6] H. Kagan,[6] R. Kass,[6] J. Lee,[6] M. Sung,[6]
A. Undrus,[6,*] R. Wanke,[6] A. Wolf,[6] M. M. Zoeller,[6] B. Nemati,[7] S. J. Richichi,[7]
W. R. Ross,[7] P. Skubic,[7] M. Wood,[7] M. Bishai,[8] J. Fast,[8] E. Gerndt,[8] J. W. Hinson,[8]
D. H. Miller,[8] E. I. Shibata,[8] I. P. J. Shipsey,[8] M. Yurko,[8] L. Gibbons,[9] S. D. Johnson,[9]
Y. Kwon,[9] S. Roberts,[9] E. H. Thorndike,[9] C. P. Jessop,[10] K. Lingel,[10] H. Marsiske,[10]
M. L. Perl,[10] S. F. Schaffner,[10] D. Ugolini,[10] R. Wang,[10] X. Zhou,[10] T. E. Coan,[11]
V. Fadeyev,[11] I. Korolkov,[11] Y. Maravin,[11] I. Narsky,[11] V. Shelkov,[11] R. Stroynowski,[11]
J. Staeck,[11] I. Volobouev,[11] J. Ye,[11] M. Artuso,[12] A. Efimov,[12] M. Gao,[12] M. Goldberg,[12]
R. Greene,[12] F. Frasconi,[12] D. He,[12] S. Kopp,[12] G. C. Moneti,[12] R. Mountain,[12]
Y. Mukhin,[12] S. Schuh,[12] T. Skwarnicki,[12] S. Stone,[12] X. Xing,[12] J. Bartelt,[13]
S. E. Csorna,[13] V. Jain,[13] S. Marka,[13] A. Freyberger,[14] R. Godang,[14] D. Gibaut,[14]
K. Kinoshita,[14] I. C. Lai,[14] P. Pomianowski,[14] S. Schrenk,[14] G. Bonvicini,[15] D. Cinabro,[15]
L. Perera,[15] B. Barish,[16] M. Chadha,[16] S. Chan,[16] G. Eigen,[16] J. S. Miller,[16] C. O'Grady,[16]
M. Schmidtler,[16] J. Urheim,[16] A. J. Weinstein,[16] F. Würthwein,[16] D. M. Asner,[17]
D. W. Bliss,[17] W. S. Brower,[17] G. Masek,[17] H. P. Paar,[17] J. Gronberg,[18] C. M. Korte,[18]
D. J. Lange,[18] R. Kutschke,[18] S. Menary,[18] R. J. Morrison,[18] S. Nakanishi,[18]
H. N. Nelson,[18] T. K. Nelson,[18] C. Qiao,[18] J. D. Richman,[18] D. Roberts,[18] A. Ryd,[18]
H. Tajima,[18] M. S. Witherell,[18] R. Balest,[19] B. H. Behrens,[19] K. Cho,[19] W. T. Ford,[19]
H. Park,[19] P. Rankin,[19] J. Roy,[19] J. G. Smith,[19] J. P. Alexander,[20] C. Bebek,[20]
B. E. Berger,[20] K. Berkelman,[20] K. Bloom,[20] D. G. Cassel,[20] H. A. Cho,[20]
D. M. Coffman,[20] D. S. Crowcroft,[20] M. Dickson,[20] P. S. Drell,[20] R. Ehrlich,[20] R. Elia,[20]
A. D. Foland,[20] P. Gaidarev,[20] R. S. Galik,[20] B. Gittelman,[20] S. W. Gray,[20] D. L. Hartill,[20]
B. K. Heltsley,[20] P. I. Hopman,[20] S. L. Jones,[20] J. Kandaswamy,[20] N. Katayama,[20]
P. C. Kim,[20] D. L. Kreinick,[20] T. Lee,[20] Y. Liu,[20] G. S. Ludwig,[20] J. Masui,[20]
J. Mevissen,[20] N. B. Mistry,[20] C. R. Ng,[20] E. Nordberg,[20] M. Ogg,[20,†] J. R. Patterson,[20]
D. Peterson,[20] D. Riley,[20] A. Soffer,[20] C. Ward,[20] P. Avery,[21] M. Athanas,[21] C. D. Jones,[21]
M. Lohner,[21] C. Prescott,[21] S. Yang,[21] J. Yelton,[21] J. Zheng,[21] G. Brandenburg,[22]
R. A. Briere,[22] D. Y.-J. Kim,[22] T. Liu,[22] M. Saulnier,[22] R. Wilson,[22] H. Yamamoto,[22]
T. E. Browder,[23] F. Li,[23] Y. Li,[23] J. L. Rodriguez,[23] T. Bergfeld,[24] B. I. Eisenstein,[24]
J. Ernst,[24] G. E. Gladding,[24] G. D. Gollin,[24] E. Johnson,[24] I. Karliner,[24] M. Palmer,[24]
M. Selen,[24] J. J. Thaler,[24] and K. W. Edwards[25]

[1]McGill University, Montréal, Québec, Canada H3A 2T8
and the Institute of Particle Physics, Canada

---

[*]Permanent address: BINP, RU-630090 Novosibirsk, Russia.

[†]Permanent address: University of Texas at Austin.

[2]Ithaca College, Ithaca, New York 14850
[3]University of Kansas, Lawrence, Kansas 66045
[4]University of Minnesota, Minneapolis, Minnesota 55455
[5]State University of New York at Albany, Albany, New York 12222
[6]Ohio State University, Columbus, Ohio 43210
[7]University of Oklahoma, Norman, Oklahoma 73019
[8]Purdue University, West Lafayette, Indiana 47907
[9]University of Rochester, Rochester, New York 14627
[10]Stanford Linear Accelerator Center, Stanford University, Stanford, California 94309
[11]Southern Methodist University, Dallas, Texas 75275
[12]Syracuse University, Syracuse, New York 13244
[13]Vanderbilt University, Nashville, Tennessee 37235
[14]Virginia Polytechnic Institute and State University, Blacksburg, Virginia 24061
[15]Wayne State University, Detroit, Michigan 48202
[16]California Institute of Technology, Pasadena, California 91125
[17]University of California, San Diego, La Jolla, California 92093
[18]University of California, Santa Barbara, California 93106
[19]University of Colorado, Boulder, Colorado 80309-0390
[20]Cornell University, Ithaca, New York 14853
[21]University of Florida, Gainesville, Florida 32611
[22]Harvard University, Cambridge, Massachusetts 02138
[23]University of Hawaii at Manoa, Honolulu, Hawaii 96822
[24]University of Illinois, Champaign-Urbana, Illinois 61801
[25]Carleton University, Ottawa, Ontario, Canada K1S 5B6
and the Institute of Particle Physics, Canada

Leptonic τ decays are sensitive probes of the charged weak interaction since the strong interaction plays no role in these decays. The Lorentz structure of the $\mu W \nu_\mu$ and $eW\nu_e$ currents are well established. In this paper we investigate the $\tau W \nu_\tau$ vertex.

Leptonic decays of the τ can be described by the most general four-fermion interaction hamiltonian [1–3] with the matrix element given by:

$$\mathcal{M} = 4\frac{G_F}{\sqrt{2}} \sum_{\substack{\gamma=S,V,T \\ \epsilon,\lambda=R,L}} g^\gamma_{\epsilon\lambda} \langle \ell_\epsilon | \Gamma^\gamma | \nu_\ell \rangle \langle \nu_\tau | \Gamma_\gamma | \tau_\lambda \rangle. \tag{1}$$

The Γ^γ matrices define the properties under Lorentz transformations of the two currents, and γ labels the type of interaction: Γ^S (scalar), Γ^V (vector), and Γ^T (tensor). The indices ϵ and λ label the right- or left- handedness (R or L) of the parent τ and the daughter charged lepton ℓ (μ,e) respectively. Only ten of the twelve complex coupling constants $g^\gamma_{\epsilon\lambda}$ are independent; g^T_{RR} and g^T_{LL} are linearly related to the others. In the Standard Model, these decays occur via the $V-A$ current (W_L boson). Thus, with a suitable choice for the arbitrary phase, $g^V_{LL}=1$, and all the other coupling constants are zero.

In the leptonic decays of the τ to $e\nu\nu$ and $\mu\nu\nu$, information on the decay can be extracted from the shape of the momentum distribution of the daughter charged lepton and its angular distribution relative to the parent tau spin direction. After integration over the unobserved neutrino momenta and the spin of the charged lepton, the charged lepton momentum spectrum in the tau rest frame can be written as a function of four Michel parameters ρ, η, ξ and δ (combinations of the coupling constants $g^\gamma_{\epsilon\mu}$) as:

$$\begin{aligned}\frac{1}{\Gamma}\frac{d\Gamma}{dx\,d\cos\Theta} = \frac{x^2}{2}\Bigg[&\frac{1+h(x)}{1+4\eta(m_\ell/m_\tau)}\left(12(1-x)+\frac{4\rho}{3}(8x-6)+24\eta\frac{m_\ell}{m_\tau}\frac{(1-x)}{x}\right) \\ &-\xi\cos\Theta\left(4(1-x)+\frac{4}{3}\delta(8x-6)+\frac{\alpha}{2\pi}\frac{g(x)}{x^2}\right)\Bigg]\end{aligned} \tag{2}$$

where $x = E_\ell/E_{max}$, E_ℓ is the energy of the daughter lepton ℓ, and $E_{max} = (m_\tau^2 + m_\ell^2)/2m_\tau$. The angle between the tau spin direction and the charged daughter lepton momentum vector is denoted by Θ, and the radiative corrections (to $\mathcal{O}(\alpha/\pi)$) are denoted by $h(x)$ and $g(x)$. Since the tau has no net polarization at CLEO beam energies, the $\cos\Theta$ term averages to zero and our data are sensitive only to the spectral shape Michel parameters ρ and η (ignoring spin correlationsamong the τ^+ and τ^-). In the Standard Model, $\rho = 3/4$ and $\eta = 0$. The current world average values for these parameters in tau decays are $\rho^\tau_{e\mu} = 0.730 \pm 0.019$ and $\eta^\tau_{e\mu} = -0.01 \pm 0.14$ [6].

In the absence of scalar and tensor interactions, an experimental determination of $\rho = 3/4$ excludes the mixing of right-handed and left-handed vector currents [4,5]. Assuming that the Standard Model $V-A$ coupling is dominant, a non-zero value of η indicates the presence of a scalar boson that couples to a right-handed tau and a right-handed daughter charged lepton. Interference between the scalar boson and Standard Model W boson amplitudes affects the low momentum part of the spectrum of the charged daughter lepton. This effect corresponds to a flipping of the lepton's spin; therefore it scales with the lepton mass, and is strongly suppressed in the electron spectrum. A possible scalar candidate is the charged Higgs of the Two Higgs Doublet Model. In this model, η is related to the mass m_H of the charged Higgs [7]:

$$\eta = - \frac{m_\tau m_\mu tan^2\beta}{2m_H^2}, \quad (3)$$

where β is the ratio of the vacuum expectation values of the neutral components of the two Higgs doublets.

The events used in this analysis were produced in the $e^+e^- \to \tau^+\tau^-$ reaction at the Cornell Electron Storage Ring CESR, operated at center-of-mass energy $E_{cm} \simeq 10.6$GeV. The data were collected with the CLEO II detector, described in detail in Ref. [8]. We have analyzed 3500 pb^{-1} (3.20×10^6 produced tau-pairs) of data, and we measure ρ_e^τ using the electron mode and ρ_μ^τ and η_μ^τ using the muon mode. We assume lepton universality to analyze the two modes simultaneously to measure $\rho_{e\mu}^\tau$ and $\eta_{e\mu}^\tau$. Since the parameters are extracted from the lepton momentum spectra, signal events are selected in such a way as to minimize the bias on the momentum spectra.

To isolate a $\tau\tau$ sample, we select events in which one τ decays to the $h\pi^\circ\nu$ mode (the tag), where h refers to the charged hadron (π or K). This decay mode has a large branching ratio, negligible QED backgrounds and negligible uncertainty associated with particle identification. The other τ in the event is required to have decayed to either $e\nu\nu$ or $\mu\nu\nu$.

Events are required to have two good tracks in the barrel region of the detector, $|\cos\theta| < 0.71$, where θ is the angle of the track with respect to the beam axis. We consider pairs of barrel photons with $E_\gamma >$100 MeV as π° candidates if their invariant mass lies within 3σ of the π° mass, where σ represents the experimental resolution on the effective di-photon mass.

The track further away in angle from the reconstructed π° is required to be either an electron or a muon. Electrons above 0.5 GeV/c are identified by momentum and specific ionization measurements from the tracking systems, and energy measurements from the electromagnetic calorimeter. We identify 31568 electrons with an estimated fake contamination of $(0.178 \pm 0.012)\%$. Muons above 1.5 GeV/c are identified by projecting tracks to hits beyond at least three absorption lengths of iron in the muon counters. We find 21766 muons with estimated fake muon background of $(1.08 \pm 0.07)\%$.

The Monte Carlo simulation uses efficiencies and fake rates measured from the data to set a weight expressing the probability that the track is identified as an electron or a muon. Lepton identification efficiencies are measured using $ee\gamma$, $eeee$, $\mu\mu\gamma$ and $ee\mu\mu$ events. We use the charged hadron from the tag decay, *i.e.*, the track closer in angle to the π°, to determine the fake muon spectrum, which we subtract from the signal spectrum. Fake electrons are not subtracted from the signal since the fake electron contamination is small.

Events with isolated, photon-like unused showers with $E_\gamma >$75 MeV in the barrel, and $E_\gamma >$100 MeV in the endcaps are vetoed to reduce background from multi-π° modes mimicking the tag mode. This minimization is important since the recoil mode is used to reconstruct the lepton spectrum in the pseudo rest frame as defined below. Using Monte Carlo simulation of these multi-π° modes we predict a remnant background contamination of $(1.19 \pm 0.05)\%$ in the electron final state and $(1.38 \pm 0.06)\%$ in the muon final state (after the pseudo rest frame cut described below).

QED backgrounds are suppressed by requiring that there be no more than one track with momentum greater that $0.85E_{beam}$, the total energy deposited in the calorimeter be less than $0.85E_{c.m.}$, the total visible energy exceed $0.2E_{c.m.}$ assuming all observed charged particles to be pions, and $|\vec{p_1}+\vec{p_2}|/(|\vec{p_1}|+|\vec{p_2}|) > 0.05$ where $\vec{p_{1,2}}$ are the momentum vectors of the two tracks in the event. Radiative Bhabha events are rejected by allowing no more than one identified electron. Remaining backgrounds from these sources, along with those due to two-photon annihilation, cosmic rays, beam gas interactions, off-axis beam particles and $q\overline{q}$ production (including $\Upsilon(4S) \to B\overline{B}$) are all estimated to be negligible.

The ideal Lorentz frame for measuring ρ and η simultaneously is the τ rest frame. The lepton spectrum observed in the laboratory differs from the one expected in the tau rest frame as a result of the Lorentz boost. All sensitivity to η is now restricted to the low momentum region for which muon identification at CLEO is limited. The lepton rest frame spectrum cannot be measured since the unobserved neutrinos in these events preclude the explicit reconstruction of the entire event. One can however, utilize information from the other tau produced in the $e^+e^- \to \tau^+\tau^-$ reaction to calculate the daughter lepton's momentum spectrum in the "pseudo" rest frame of its parent tau [9]. In the absence of radiation, the tau pair is produced with the two taus back-to-back and at the beam energy. We use the direction of the tag $h\pi^\circ$ system as an estimator of the flight direction of its parent tau. In the decay $\tau \to H\nu$, where H is the hadronic system and α is the angle between the τ and the daughter H system in the laboratory frame,

$$m_\tau^2 + m_H^2 - 2E_\tau E_H + 2p_\tau p_H \cos\alpha = m_\nu^2 \ . \tag{4}$$

E_H, p_H and m_H are all measured quantities. The azimuth angle of $\vec{p_H}$ about $\vec{p_\tau}$ is unknown, but its importance vanishes as $\alpha \to 0$. We assume $m_\nu = 0$ and $E_\tau = E_{beam}$ to calculate $\cos\alpha$, and since not every H tag is a good estimator, we select events with $\cos\alpha \geq 0.970$ to reconstruct the pseudo rest frame spectrum. This cut is indicated by the arrow in Fig. 1, where we display the distribution in $\cos\alpha$ of the data and the Monte Carlo simulation. After the $\cos\alpha$ requirement one retains 18587 (12580) electrons (muons). These numbers are consistent with expectations from world average branching ratios for the leptonic decay modes and the $h\pi^\circ\,\nu$ decay mode.

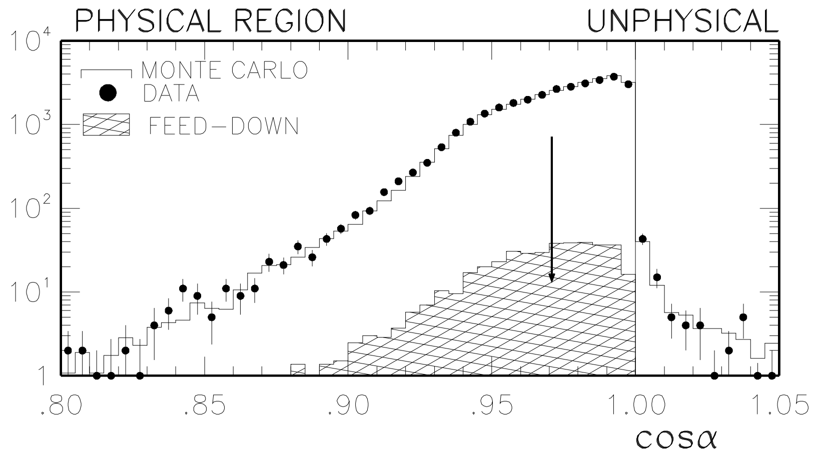

FIG. 1. $\cos\alpha$ as calculated from Eq. 4 for the data (dots) as well as the generic tau Monte Carlo simulation (solid histogram). The arrow indicates the nominal minimum requirement. Background from multi-π° decay modes is included in the simulations in the appropriate proportions (hatched region). There are events in both the data and the Monte Carlo simulation which have $\cos\alpha > 1$, an unphysical region. These events result from measurement errors and are discarded.

In the pseudo rest frame we recover 2931 additional muons that lie below the 1.5 GeV/c laboratory momentum threshold of the muon identification system. These muons are identified kinematically by elimination of all other possible decay hypotheses ($\pi\nu$, $K\nu$, $e\nu\bar{\nu}$, and $hn\pi^0\nu$). The scaled pseudo rest frame energy, $X = E_\mu/E_{\rm MAX}$, where E_μ is the muon energy in the pseudo rest frame and $E_{\rm MAX} = (m_\mu^2 + m_\tau^2)/2m_\tau$ is shown in Fig. 2 for muons with a laboratory frame momentum $0.5 < p_\mu < 1.5$ GeV/c. The $p_\mu \geq 0.5$ GeV /c momentum requirement is essential for good electron identification, which is used to veto electron-like events, thus reducing the electron contamination to $(0.64 \pm 0.11)\%$. For the two-body modes $\pi\nu$ and $K\nu$ we have $E_{(\pi,K)} = (m_\tau^2 + m_{(\pi,K)}^2)/2m_\tau$, corresponding to $x_{\pi(K)} = 0.89(0.95)$ in the true rest frame , and the $X \leq 0.6$ cut indicated in the figure reduces the π, K contamination to $(2.63 \pm 0.21)\%$. No extra unmatched showers with E_γ >60 MeV are allowed either in the barrel or the endcap region to minimize backgrounds from $h\pi^\circ\,\nu$ and other multi-pizero modes; this contamination is estimated to be $(0.78 \pm 0.12)\%$. These backgrounds to the low momentum muon signal are calculated with the Monte Carlo simulation and subtracted from the data. We recover a small but pure sample of muons with $0.5 < p_\mu < 1.5$ GeV/c and $X \leq 0.6$, highly sensitive to the η parameter.

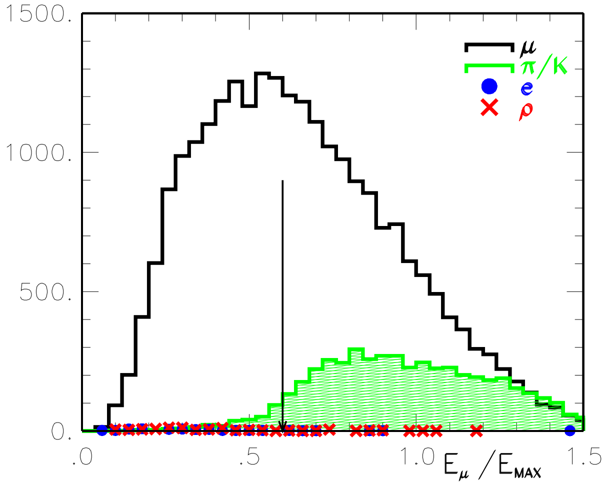

FIG. 2. The scaled pseudo rest frame muon energy spectrum obtained from the Monte Carlo simulation, for muons with a laboratory frame momentum $0.5 < p_\mu < 1.5$ GeV/c , are shown here. The Monte Carlo spectra for all the possible background modes are also indicated in this figure and we note that the contributions from all possible background modes are small in the $X < 0.6$ region indicated by the arrow.

The observed charged daughter lepton spectrum, integrated over the two undetected neutrino momenta and averaged over the tau spin direction, can be expressed in terms of three Monte Carlo spectra; the standard $V - A[\rho = 3/4, \eta = 0]$ spectrum, the $V + A[\rho = 0, \eta = 0]$ spectrum and the $\eta = 1[\rho = 3/4, \eta = 1]$ spectrum:

$$\frac{d\Gamma_{obs}}{dx}(\rho,\eta) = \left(\frac{1}{N}\right)\left(\left[\frac{(4\rho/3-\eta)(\epsilon_{\rm V\text{-}A})}{1+4\eta(m_\ell/m_\tau)}\right]\frac{d\Gamma}{dx}(3/4,0) + \left[\frac{(1-4\rho/3)(\epsilon_{\rm V+A})}{1+4\eta(m_\ell/m_\tau)}\right]\frac{d\Gamma}{dx}(0,0) \right.$$
$$\left. + \left[\frac{\eta(1+4(m_\ell/m_\tau))(\epsilon_{\eta=1})}{1+4\eta(m_\ell/m_\tau)}\right]\frac{d\Gamma}{dx}(3/4,1)\right) \qquad (5)$$

The overall reconstruction efficiencies for the three Monte Carlo samples are $\epsilon_{\text{V-A}}, \epsilon_{\text{V+A}}$ and $\epsilon_{\eta=1}$. The momentum cut-off dictated by lepton identification criteria in both of the leptonic modes results in the different efficiencies for each spectrum. N is the sum over the terms in the square brackets preceding the three different Monte Carlo distributions. The Monte Carlo spectra are individually normalized to the total number of data events. Since the coefficients in Eq. 5 sum to unity, the fit function integrates to the total number of observed events for all relevant values of the parameters.

The lepton momentum spectrum in the data is now fit to the above function of three binned Monte Carlo momentum spectra generated with the values of ρ and η given above. We use the KORALB(v2.2) [10]/TAUOLA(v2.4) [11]/PHOTOS(v1.06) [12] Monte Carlo packages to model the production and decay of tau pairs, and the GEANT 3.15 [13] program to simulate the response of the CLEO detector. Small modifications to the TAUOLA package were required to generate decays with arbitrary values of η and ρ [14]. All effects due to radiation, resolution and efficiency are included in the three Monte Carlo spectra.

In the electronic decay mode, all sensitivity to the η parameter is lost as $m_e \ll m_\tau$. This is equivalent to setting $\eta = 0$, its Standard Model expectation. The electron data are analyzed with one free parameter, ρ. We measure $\rho_e^\tau = 0.734 \pm 0.017$ with a χ^2 of 51.5 for 46 degrees of freedom. The laboratory frame momentum spectrum used in this fit is illustrated in Fig. 3(a). In the pseudo rest frame, the improvement in sensitivity to ρ is offset by the loss in statistical precision resulting from the $\cos\alpha$ requirement. The result obtained using this frame is essentially identical to the laboratory frame result.

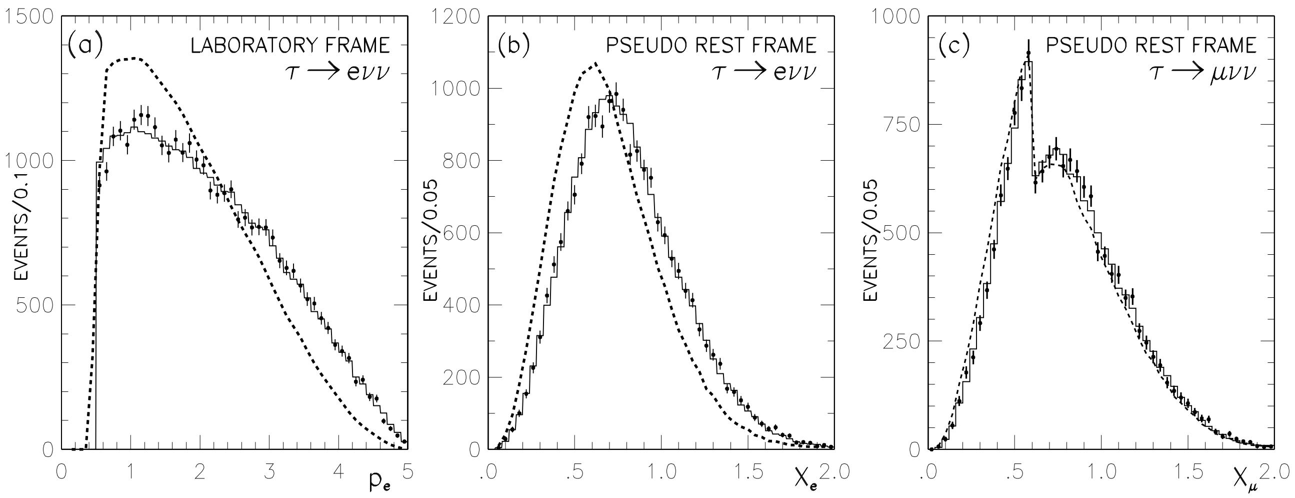

FIG. 3. The electron laboratory frame spectrum shown in (a) is used to measure ρ_e, and the electron and muon pseudo rest frame scaled momentum spectra shown in (b) and (c) are used for the simultaneous measurement of ρ and η. The addition of the low momentum muons results in the discontinuity observed at $X_\mu = 0.6$ in (c). Events with $X > 1$ in the pseudo rest frame spectra occur primarily because of the imperfect reconstruction of the τ direction. The dots represent the data, and the solid histogram represents the fit function. The dotted lines in (a) and (b) represent the electron $V + A$ Monte Carlo spectrum in the laboratory and pseudo rest frames respectively, and the dotted line in (c) represents the muon $\eta = 1$ Monte Carlo spectrum in the pseudo rest frame.

In the muon mode, the two parameters are strongly correlated and we measure them simultaneously using the pseudo rest frame spectrum as illustrated in Fig. 3(c); $\rho^\tau_\mu = 0.780 \pm 0.055$ and $\eta^\tau_\mu = 0.14 \pm 0.18$. The χ^2 resulting from the fit is 26.9 for 34 degrees of freedom, and the correlation coefficient $C_{\rho\eta}$, is 0.943. Neglecting the low momentum muons recovered without conventional muon identification, results in significantly larger errors. Results obtained on analyzing the laboratory frame spectrum are consistent with the pseudo rest frame fits, but the errors are $\simeq 60\%$ larger.

The high precision on ρ obtained in the electron mode analysis is now used to help constrain the η parameter by a simultaneous pseudo rest frame fit to both modes (Figs. 3(b) and 3(c)). Invoking lepton universality, we measure $\rho^\tau_{e\mu} = 0.739 \pm 0.016$, $\eta^\tau_{e\mu} = 0.025 \pm 0.074$ with $C_{\rho\eta} = 0.638$, and the χ^2 is 69.5 for 75 degrees of freedom. Once again the laboratory frame results are consistent with these results. We show in Fig. 4 results of the combined pseudo rest frame fit, along with the measurements from the individual modes.

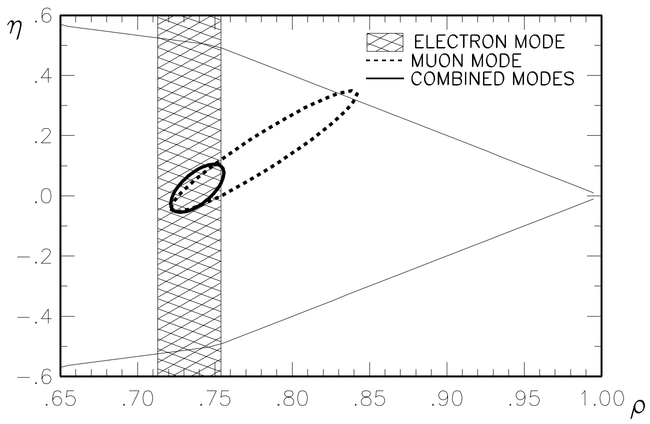

FIG. 4. The large dotted contour indicates the 1σ error ellipse obtained in the $\eta - \rho$ plane from the muon data. The shaded band indicates the corresponding result obtained with the electron mode, and the small dark ellipse indicates the 1σ result obtained from the simultaneous fit to both modes with the universality assumption. All results are consistent with the Standard Model expectations and lie well within the solid lines which enclose the allowed region in $\eta - \rho$ space.

Table I lists the systematic error contributions. We find that in spite of the very large sample used, this measurement is statistics limited. The complete CLEO Monte Carlo simulation is used to determine the efficiencies of all applied cuts, along with their effects on the required momentum distribution; the data are used to tune the Monte Carlo simulation wherever possible.

Lepton identification efficiencies measured from the data, are used in the Monte Carlo, and statistical uncertainties in these measurements lead to small systematic errors in the present measurements. Our $p_\mu > 1.5$ GeV/c momentum cut-off, for muons identified by penetration, ensures that the identification efficiency is well modeled.

The trigger efficiencies are close to 100% in both modes and most events satisfy multiple trigger paths. The absolute trigger efficiency varied by as much as 2% during the data collection. These changes are momentum independent and the systematic error contributions resulting from the trigger are small.

Background levels, given in the event selection discussion above, are small for all sources. Both the normalization and the momentum dependence of each significant background source is varied within allowed ranges to estimate the systematic contributions from that source.

The extra energy veto applied to minimize the multi-π° background also discards signal events with radiative photons and showers resulting from hadronic interactions in the calorimeter. These effects are included in the Monte Carlo simulation, but not perfectly. We estimate the resulting systematic errors by calculating the parameters for different veto requirements *i.e.*, by changing the amount of background allowed in the sample.

Detector and global cuts, spin correlations and radiation all correlate the signal and tag tau decays in the event. All these effects are modeled in the Monte Carlo, and any systematic errors arising from an imperfect modeling of these effects are studied by imposing and varying requirements on the recoil tau decay.

High momentum tracks can be mismeasured by as much as 50-100 MeV/c, and bin migration can potentially alter the observed spectrum shape. Since all the fits performed utilize 100 MeV/c bins, the systematic errors associated with binning effects are small. This has been confirmed by measuring all the parameters with a large range of bin sizes.

Radiation effects are important as we are looking for small deviations from the Standard Model. Initial and final state radiation have the largest rate and the greatest potential to distort the momentum spectrum. We evaluate the systematic error contribution from this source by varying the radiation-weighted Monte Carlo spectrum by as much as $\pm10\%$ in the fits performed to extract the two parameters. The contribution from decay radiation photons in $\tau \rightarrow \ell\nu\nu\gamma$ as well as from photons resulting from external bremsstrahlung in the detector material are negligible.

TABLE I. All significant sources of errors

SOURCE	e MODE	μ MODE		$e+\mu$ MODES	
	ρ_e	ρ_μ	η_μ	$\rho_{e\mu}$	$\eta_{e\mu}$
Electron ID	<0.001	–	–	<0.001	0.001
Muon ID	–	0.004	0.018	0.001	0.024
Fake electron	0.004	–	–	0.004	0.015
Fake muon	–	0.011	0.046	<0.001	0.011
Feed-down	0.001	0.002	0.007	0.002	0.008
Trigger	0.002	0.006	0.019	0.002	0.005
Veto Cuts	0.006	0.023	0.057	0.008	0.040
Tag-Signal Correlations	0.003	0.025	0.101	0.005	0.025
Bin Migration	0.001	0.020	0.100	0.001	0.016
Radiation	0.005	0.003	0.050	0.001	0.004
MC Statistics	0.006	0.025	0.088	0.006	0.030
Total Systematics	0.011	0.048	0.191	0.013	0.066
Data Statistics	0.017	0.055	0.181	0.016	0.074

QQ generator level tests were carried out to study the performance of the fitting procedure. We find that the fitter tracks both parameters over their respective allowed ranges in parameter space; there is no systematic bias associated with the fitting procedure.

Each of the Monte Carlo samples used in this analysis is approximately a factor of 10 larger than the data in size. Yet, Monte Carlo statistics remains one of the largest sources of systematic error.

The results obtained for the different parameters measured, along with the current world average measurements, are presented in Table II. Since the two parameters are strongly correlated, all of these results (except ρ_e) are obtained from simultaneous two parameter fits. The world averages exclude measurements obtained with one parameter fixed.

All the results presented here are consistent with previous measurements and theoretical expectations based on the Standard Model. The errors on these results are approximately half the corresponding errors obtained by previous measurements and are comparable to or lower than the present world average errors. This measurement of the η parameter provides via Eq. 3 a lower limit on the charged Higgs mass: $M_{H^\pm} > (0.71 \times \tan\beta)$ GeV at the 90% confidence level.

TABLE II. Results obtained in this analysis along with the current world average results.

Parameter	This Result	Previous World Average
ρ^τ_e	$0.734 \pm 0.017 \pm 0.011$	0.741 ± 0.025
ρ^τ_μ	$0.780 \pm 0.055 \pm 0.048$	0.697 ± 0.056
η^τ_μ	$0.140 \pm 0.181 \pm 0.191$	-0.156 ± 0.238
$\rho^\tau_{e\mu}$	$0.739 \pm 0.016 \pm 0.013$	0.730 ± 0.019
$\eta^\tau_{e\mu}$	$0.025 \pm 0.074 \pm 0.066$	-0.01 ± 0.14

We gratefully acknowledge the effort of the CESR staff in providing us with excellent luminosity and running conditions. J.P.A., J.R.P., and I.P.J.S. thank the NYI program of the NSF, M.S thanks the PFF program of the NSyF, G.E. thanks the Heisenberg Foundation, K.K.G., M.S., H.N.N., T.S., and H.Y. thank the OJI program of DOE, J.R.P, K.H., and M.S. thank the A.P. Sloan Foundation, and A.W., and R.W. thank the Alexander von Humboldt Stiftung for support. This work was supported by the National Science Foundation, the U.S. Department of Energy, and the Natural Sciences and Engineering Research Council of Canada.

REFERENCES

[1] L. Michel, Proc. Phys. Soc. **A63** (1950) 514.
[2] T. Kinoshita and A. Sirlin, Phys. Rev. **107** (1957) 593.
[3] C. Bouchiat and L. Michel, Phys. Rev. **107** (1957) 170.
[4] F. Scheck, Phys. Rep. **44** (1978) 187.
[5] W. Fetscher, Phys. Rev. **42** (1990) 1544.
[6] M. Davier, Nuclear Physics B (proc. Suppl.) **40** (1995) 395-412
[7] A. Stahl, Phys. Lett. **B 324** (1994) 121-124.
[8] CLEO Collaboration, Y. Kubota *et al*, Nucl. Instrum. Methods Phys. Res., Sect. A **320** (1992) 66.
[9] ARGUS Collab, H. Albrecht et al., Phys. Lett. **B 341** (1995) 441-447
[10] S. Jadach and Z. Was, Comput. Phys. Commun. **36** (1985) 191 .
[11] S. Jadach, J. H. Kuhn and Z. Was, CERN-TH-5856/90 (1990).
[12] E. Barberio, B. van Eijk and Z. Was, CERN-TH-5857/90 (1990).
[13] R. Brun *et al*, CERN dd/ee/84-1.
[14] M. Schmidtler, IEKP-KA/93-14, A Convenient Parametrization for the General Matrix Element of Leptonic Tau Decays (1993).